The Nearby Field Galaxy Survey

A spectrophotometric and photometric study of nearby galaxies

Rolf A. Jansen[1,2] (jansen@astro.rug.nl)
[1] *Kapteyn Astronomical Institute, Postbus 800, NL-9700 AV Groningen, The Netherlands*

Sheila J. Kannappan[2] (skannappan@cfa.harvard.edu)
[2] *Harvard-Smithsonian Center for Astrophysics, Cambridge, MA 02138, U.S.A.*

Abstract.
We report on our observing program to obtain integrated spectrophotometry, intermediate and high resolution major axis spectra, and UBR surface photometry of a representative sample of ∼200 galaxies in the nearby field. The main goal of this program is to provide a comparison sample for high redshift studies and to study the variation in star formation rates (SFR), star formation history (SFH), excitation, metallicity, and internal kinematics over a large range in galaxy luminosity and morphological type. In particular, we extend the work of Kennicutt (1992) to lower luminosity systems.

We present the main results of our analysis sofar. In these proceedings, we condense the presented two atlases of (1) images and radial surface brightness profiles and color profiles, and (2) of images and integrated spectra into several example images, profiles and spectra, showing the general trends observed. For the original atlasses we refer to the electronic distribution on CDROM or as available on the Web at http://www.astro.rug.nl/∼nfgs/.

1. Introduction

As galaxies are now routinely sampled at fainter magnitudes and higher redshifts than ever before, one of the major problems with the interpretation of distant spectroscopic data has become the difficulty of obtaining good comparison samples in the local universe. Distant galaxies subtend a small angle on the sky and their spectra are unavoidably integrated spectra, while most spectra of nearby galaxies are nuclear spectra only. A direct comparison of distant and nearby galaxy spectra, therefore, is difficult.

In a pioneering effort, Kennicutt (1992) obtained integrated spectrophotometry for 90 galaxies spanning the entire Hubble sequence. His study has been a benchmark for the interpretation of spectra at both high and low redshift. The range in luminosity sampled per type, however, was limited to the brightest galaxies, and no uniform surface photometry nor internal kinematical data is available. Also, only 44 out of 90 galaxies were observed at intermediate spectral resolution (5–7Å), the remainder at lower resolution (15–20Å). Large homogeneous samples of intermediate or high resolution nuclear and integrated spectrophotometry, supplemented by multi-filter surface photometry, for galaxies spanning the entire Hubble sequence and with a large range in luminosity, are absent in the literature to date.

2. The Nearby Field Galaxy Survey

With our Nearby Field Galaxy Survey (NFGS) we aim to remedy this situation. The purpose of our study is to obtain integrated and nuclear spectrophotometry over the entire optical regime, as well as U, B, R, H and K' surface photometry, and high resolution spectroscopy, for a sample of 196 galaxies in the nearby field, including galaxies of all types and spanning a large range in luminosity. With "field" we imply a selection that includes galaxies in clusters, groups an low density environments, as opposed to a selection favoring any single one of these.

The data will be used to study the emission and absorption line strengths, star formation rate and star formation history, morphologies, structural parameters, colours, magnitudes and internal kinematics of gas and stars, both globally and as a function of radius within a galaxy. We thus aim to extend the work of Kennicutt to lower luminosity galaxies accross the Hubble sequence and to study the variation in galaxy properties over a large range in absolute magnitude and type.

The data can be used as a benchmark for galaxy evolution modelling and comparison with observations of high redshift galaxies, as will result from future observations with large ground-based telescopes and the NGST.

3. Selection of the sample

The 196 target galaxies in this survey have been objectively selected from the CfA redshift catalog (CfA I, Huchra et al. 1983) to span the full range in absolute B magnitude present in CfA I ($-14 < \mathrm{M}_B < -22$), while sampling fairly the changing mix of morphological types as a function of luminosity. Absolute magnitudes were calculated directly from blue photografic magnitudes and radial velocities in the Local Group rest-frame, assuming $\mathrm{H}_0 = 100$ km s^{-1} Mpc^{-1}.

To avoid a sampling bias favoring a cluster population we excluded galaxies in the direction of the Virgo Cluster with velocities smaller than 2000 km sec^{-1}. We also minimized the number of galaxies larger than 3 arcmin (the slit length of the FAST spectrograph) by imposing a luminosity dependent lower limit on the radial velocity. Thus, we do not impose a strict diameter limit, while avoiding selecting the nearest high luminosity galaxies (which tend to be the largest on the sky). We sorted the 1006 galaxies remaining after our Virgo Cluster and radial velocity cuts into 1 magnitude wide bins of absolute magnitude, which in turn were sorted according to Hubble type. We then drew from each bin a number of galaxies chosen to approximately reproduce the local galaxy luminosity function, while preserving the mix of morphological types in each luminosity bin. The total number of galaxies selected is 196, with a median redshift of 0.01 and a maximum redshift of 0.07 . Only 8 of these have major axis optical diameters larger than the slit length.

In Figure 1 we give an overview of the global properties of the selected galaxy sample. The number distributions in magnitude, type and color are broad and, although the distribution in effective surface brightness is peaked, we do have several examples of low surface brightness galaxies.

With very few caveats this sample can be considered a fair representation of the local galaxy population.

4. Observations

4.1. *UBR* Surface photometry

The photometric observations were obtained at the F.L. Whipple Observatory's 1.2 m telescope[1] during 50 dark nights between 1994 March and 1997 March. U filter images were obtained with a thinned backside illuminated CCD, while most B and R images were obtained with an older camera and a front illuminated CCD. Typically, we exposed 2×450, 2×900 and 1×900 seconds to reach limiting surface brightnesses of $\mu_R = 26.1$, $\mu_B = 27.2$, and $\mu_U = 26.7$ mag arcsec^{-1} in R, B, and U.

Radial surface brightness profiles were extracted using an ellipse fitting procedure (Jørgensen, Franx & Kjærgaard 1992) with center, position angle and ellipticity fixed at all radii to the average values in the outer parts. Total, effective and isophotal magnitudes were calculated from the radial surface brightness profiles. Tests of the internal and external accuracy of our photometry indicate typical errors of 0.02 mag and 0.05 mag for isophotal and total magnitudes, respectively.

[1] The F.L. Whipple Observatory (FLWO) is operated by the Smithsonian Astrophysical Observatory, and is located on Mt. Hopkins in Arizona.

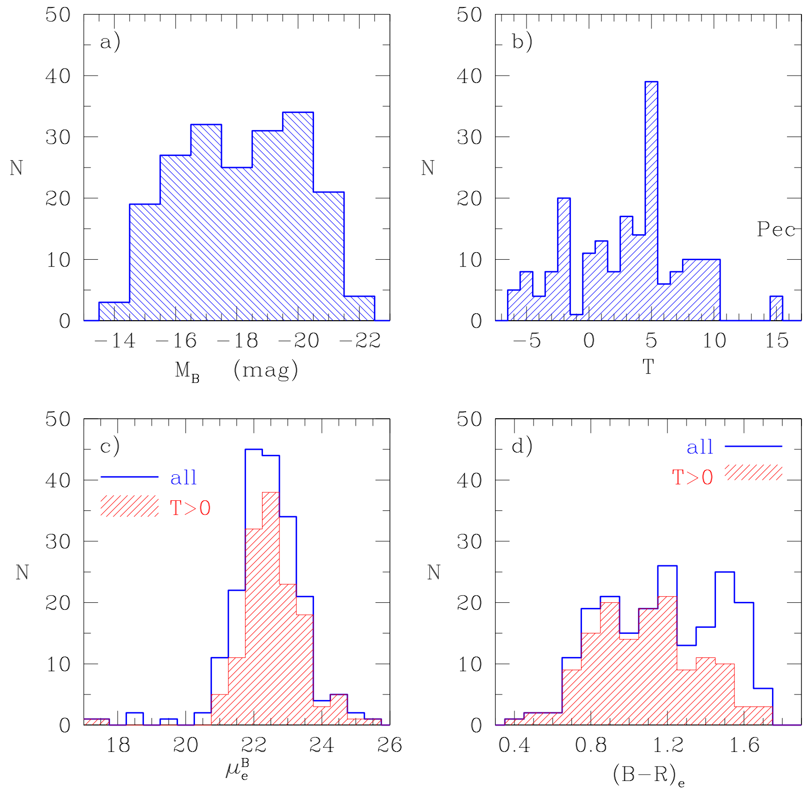

Figure 1. Overview of the global properties of the selected galaxy sample. Presented are the number distributions as a function of: a) absolute B magnitude; b) numeric galaxy type (note that we choose to place the unclassified early type galaxies at T= -4 (cD) rather than -7, as we do not have any cD galaxies in our sample, and this placement seems more natural with respect to the compact ellipticals at T= -6); c) the surface brightness at the effective radius in B; and d) the effective $(B-R)$ color, measured within that effective radius. In panels c) and d) the open histograms represent the selected sample, and the shaded ones the subsample of galaxies with types later than S0/a.

4.2. Spectrophotometry

Integrated and nuclear spectra were obtained with the FAST spectrograph (Fabricant et al. 1998) at the FLWO 1.5 m telescope during 41 nights between 1995 March and 1997 March. The 2720×512 pixel thinned CCD of the FAST in combination with a 300 l/mm grating allowed coverage of the entire near-UV through optical range (3500–7250Å) in a single exposure, at a resolution (FWHM) of ~6Å. We approximately aligned the spectrograph slit with the major axis of each galaxy. The integrated spectra were obtained by drift scanning

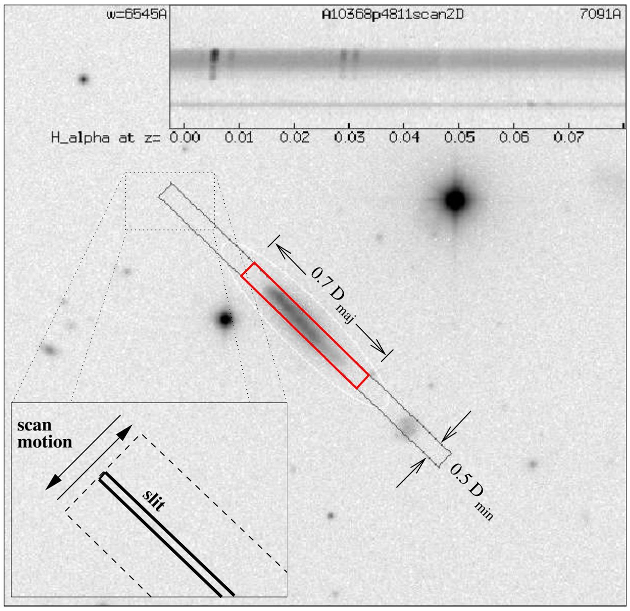

Figure 2. Example of the geometry of the periodic drift scan to obtain integrated spectra. The total distance over which the slit is moved back and forth is half the blue minor axis optical diameter. This distance was chosen to match the expected surface brightness limit of the 1.5 m telescope and FAST spectrograph. The spectra were extracted into 1-D spectra using an objectively defined aperture of size 0.7 times the major axis diameter at $\mu_B = 26$ mag arcsec^{-1}, as determined from our B filter photometry. The ellipse drawn into the image was fit to the B_{26} isophote. In the case of galaxy A10368+4811, we sample ∼80% of the light within this isophote, or 68% of the total galaxian light.

the slit over a total distance of half the minor axis optical diameter and extracting over 0.7 times the major axis optical diameter (Figure 2). Thus, on average, we sample almost 80% of the total galaxy light.

Based on a comparison of the $(B-R)$ colors measured in our photometry and the synthetic colors measured in the spectra, and on a comparison with several galaxies from Kennicutt's sample reobserved for this goal, we claim an overal relative spectrophotometric accuracy of 6%.

4.3. Internal kinematics

Kannappan et al. (in prep.) have obtained high resolution spectra in the range 6000–7000Å (emission line galaxies) at a resolution (FWHM) of 1Å, and in the range 4000–6000Å (no or relatively little emission) at a resolution (FWHM) of 2.3Å. Rotation curves were derived from the former (see Figure 3) by simultaneously fitting the wavelengths of Hα,

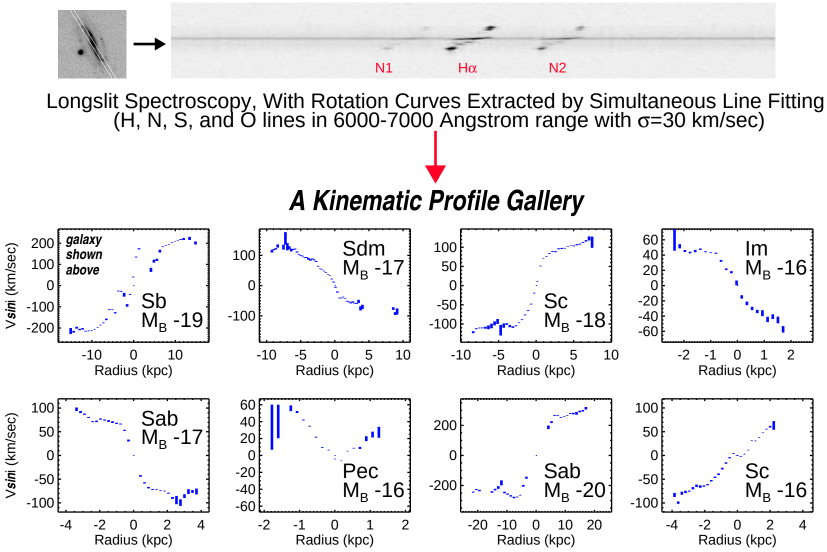

Figure 3. Gallery of several example optical rotation curves. At top left, a greyscale B filter image is given for one galaxy with the orientation of the spectrograph slit indicated. The resulting 2-D spectrum image, spanning the range 6000–7000Å in wavelength, is presented with the strongest emission lines marked. The extracted rotation curve for this galaxy is presented in the upper left panel of the gallery, showing that this galaxy is similar in size, luminosity and mass to our own Milky Way galaxy.

[NII], [SII] and [OI] lines as a function of radius in a galaxy. Velocity dispersions were fit using a velocity broadened stellar template and a Fourier fitting algorithm (Franx, Illingworth, & Heckman 1989) in the latter spectra.

The main goals of these measurements are to study galaxy mass profiles as a function of morphological and spectrophotometric properties, to compare gas and stellar kinematics, and investigate kinematic evidence of galaxy interactions, mergers and mass infall.

4.4. H AND K' SURFACE PHOTOMETRY

We are currently obtaining H and K' filter surface photometry for the NFGS galaxies (Pahre et al. (in prep.)) to determine the relative contributions of spheroids and disks to the luminosity density of the local universe. Near-infrared data for half the sample are now available.

Previous measurement of this parameter (Schechter & Dressler 1987) relied on visual total magnitude and bulge estimates from photographic plates and suffered from relatively poor knowledge of the luminosity functions of different morphological types. Combination of U, B, R, H

and K' photometry and our spectrophotometry will allow a better separation of age and metallicity effects, as well as internal extinction, while inversion of our selection and comparison with a deeper complete spectroscopic sample (Carter et al. (in prep.)) allows us to infer volume densities as a function of type and luminosity.

5. Results

5.1. Surface photometry

We observe a strong trend of $(B-R)_e$ color with morphological type, with later type galaxies becoming progressively bluer (Figure 4a). The observed scatter on this trend is 0.19 mag, which is smaller than the 0.24 mag scatter on the color–magnitude trend where intrinsically fainter systems tend to be bluer than brighter systems (Figure 4b). Estimating a galaxy's broad type class (E,S,Irr) from its color can, therefore, be as accurate as estimates based on galaxy asymmetry and central concentration of the light (Abraham et al. 1996).

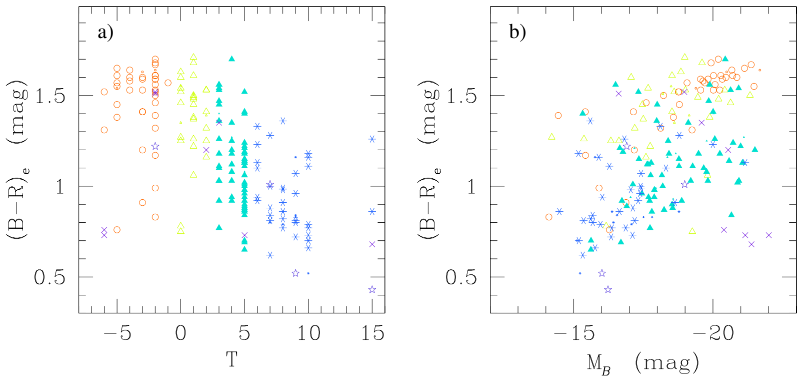

Figure 4. Effective $(B-R)$ colors as a function of morphological type and absolute B magnitude. Points are coded according to type as follows. Ellipticals and S0's (T $<$ 0) are indicated by open circles, early type spirals ($0 \leq$ T < 3) by open triangles, intermediate spirals ($3 \leq$ T < 6) by solid triangles, and late type spirals and irregulars by asterixes. Active nucleated galaxies are indicated by crosses and starburst galaxies by open stars.

We find that color–magnitude relations are useful for early type systems and to a lesser degree for very late type systems, but not useful for intermediate type spirals. We also verify the result of Tully et al. (1996), that the faintest galaxies may become redder with radius instead of bluer. Star formation is the driving force in this trend (Jansen et al. 1999a).

5.2. Spectrophotometry

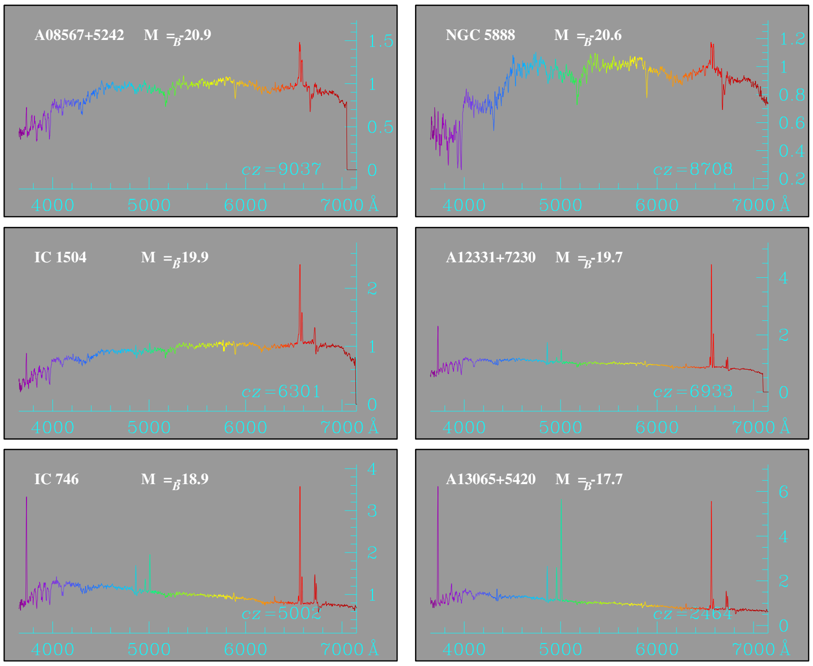

Figure 5. Gallery of spectrophotometrically calibrated integrated spectra as a function of luminosity for 6 Sb galaxies. At all Hubble types, continua tend to become bluer and the percentage of galaxies showing emission increases going to fainter luminosities. The range in spectral properties at each type and luminosity appears to be large, however.

The bluing of galaxies towards both later morphological types and lower luminosities is apparent in the spectrum continua (Figure 5) as well. Moreover, the emission line strengths increase with respect to the continua going to lower luminosity systems. This trends is most apparent for the intermediate type spiral galaxies, but can be seen all accross the Hubble sequence.

Of particular interest is the relative strength of the [OII]3727Å line with respect to Hα, as [OII] is the strongest line available in the optical regime for galaxies with $0.3 \lesssim z \lesssim 1$ and has been widely used as a tracer of the SFR. Both figures 5 and 6b show that the fainter galaxies tend to have [OII] in excess of the relation found by Kennicutt (1992), corresponding to EW([OII])$\simeq$ 0.6 EW(Hα). Preliminary analysis indicates that this must be attributed to a combination of (1) a higher average excitation temperature in the ISM of faint galaxies — which in turn is due to their lower metallicities — which boosts the strenght of [OII] relative to the Balmer lines over a large range in temperature, and (2) a lower interstellar extinction or smaller filling factor of obscuring matter than derived for high luminosity systems.

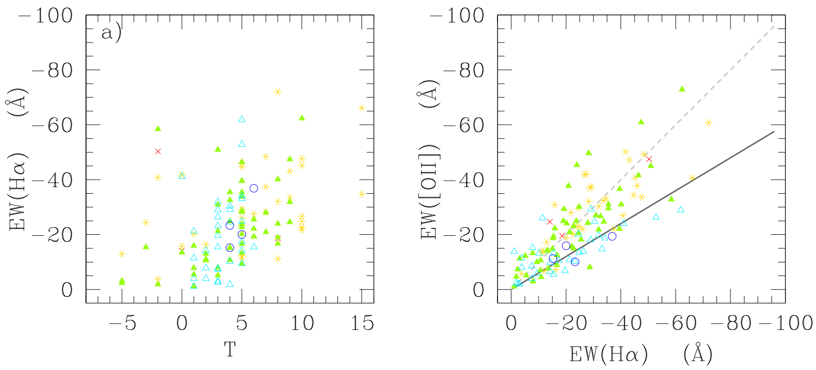

Figure 6. Integrated emission line strengths for the 122 normal star forming galaxies with EW(Hα)>1Å. Symbols are coded according to total *B* filter luminosity, from high to low, as open circles, open triangles, solid triangles, asterixes and crosses. a) Hα equivalent widths versus type. b) [OII]3727Å versus Hα equivalent widths. High luminosity galaxies follow the relation found by Kennicutt (1992; solid line), while galaxies fainter than $M_B \sim -19$ tend to follow a much steeper relation, approximating even EW(Hα) (cf. the line of equality (dashed)).

References

Abraham, R.G., Tanvir, N.R., Santiago, B.X., Ellis, R.S., Glazebrook, K., & van den Bergh, S., 1996, MNRAS, 279, L47

Carter, B., Fabricant, D.G., et al., (in prep.)

Fabricant, D., Cheimets, P., Caldwell, N., & Geary, J., 1998, PASP, 110, 79

Franx, M., Illingworth, G., & Heckman, T., 1989, AJ, 98, 538

Hammer, F., Flores, H., Lilly, S.J., Crampton, D., Le Fèvre, O., Rola, C., Mallen-Ornelas, G., Schade, D., & Tresse, L., 1997, ApJ, 481, 49 (CFRS XIV)

Huchra, J.P., Davis, M., Latham, D., & Tonry, J., 1983, ApJS, 52, 89 (CfA I)

Jansen, R.A., Franx, M., Fabricant, D.G., & Caldwell, N., 1999a (ApJS, in prep.)

Jansen, R.A., Fabricant, D.G., Franx, M., & Caldwell, N., 1999b (ApJS, in prep.)

Jansen, R.A., Franx, M., Fabricant, D.G., & Caldwell, N., 1999c (Ph.D. thesis, University of Groningen)

Jørgensen, I., Franx, M., & Kjærgaard, P., 1992, A&AS, 95, 489

Kannappan, S.J., Fabricant, D.G., & Franx, M., (in prep.)

Kennicutt, R.C. Jr., 1992, ApJ, 388, 310

Pahre, M., Jansen, R.A., Kannappan, S.J., Fabricant, D.G., & Willner, S., (in prep.)

Schechter, P.L., & Dressler, A. 1987, AJ, 94, 563

Tully, R.B., Verheijen, M.A.W., Pierce, M.J., Huang, J.-S., & Wainscoat, R., 1996, AJ, 112, 2471